Ground-based infrared remote sensing based on the height of middle and low cloud

SUN Xuejin, QIN Chao, QIN Jian, LIU Lei, HU Yuning

Institute of Meteorology, *PLA University of Science & Technology*, *Nanjing* 211101, *China*

Abstract: Based on the analysis of results of radiative transfer simulation, a method for ground-based infrared remote sensing of cloud based on height is proposed according to the monotonic relationship between Cloud Base Height (CBH) and the downwelling infrared radiance. A preliminary comparison experiment is conducted with cloud base height measured by laser ceilometers. The results show high accuracy of CBH of middle and low cloud determined according to the proposed method with an average error of 107 m.

Key words: cloud base height, infrared remote sensing, downwelling infrared radiance, ground-based remote sensing, laser ceilometer

1　INTRODUCTION

Clouds are one of the most important moderators of the earth-atmosphere radiation budget. They affect the earth-atmosphere radiation balance by the reflection and absorption of solar and terrestrial radiation and are observed by artificial visual for a long time at weather stations. Satellite cloud imageries have been obtained by meteorological satellites since 1960's and they play an important role on the study of global cloud distribution and change. However, it can not fully meet the needs of atmospheric research for its poor capacity of inversion of CBH and detection of lower cloud for multi-layer clouds. It shows that CBH is important in the study of the energy budget of Earth's long-wave radiation. In addition, the accuracy of satellite remote sensing data needs to be verified by the ground-based dataset, which makes the ground-based cloud observation necessary.

Visual observation is the key method of the ground-based cloud observation, but it cannot provide objective data with high time resolution and the same accuracy from day to night. Laser ceilometers are used to measure CBH for some years. However, they can only make single-point observation, and cloud amount or some other cloud characters cannot be retrieved. In addition, laser ceilometers are strongly influenced by aerosols which restrict their operational uses. With the development of digital technology, a variety of visible light digital imaging devices have been developed, such as the Total Sky Imager(TSI) (Long & DeLuisi, 1998), Whole Sky Imager(WSI)(Shields, et al., 1998), and All-sky Digital Camera (Huo & Lv, 2002). Images obtained by some of these devices can-

not be further analyzed to retrieve cloud amount during the night. As to some other devices, it hardly achieves the same accuracy of cloud identification from day to night because of the different cloud identification algorithms. Over the last decade, with development of the infrared measurement technology, the thermal infrared technology for cloud remote sensing has been developed, such as Infra-red Cloud Analyzer (Genkova, et al., 2004), Infrared Cloud Imager (Shaw, et al., 2002) and Whole Sky Infrared cloud Measuring System(WSIRCMS) (Sun, et al., 2008a). Cloud amount and some other characters such as cloud-base height can be obtained by such ground-based infrared remote sensing devices during both day and night.

WSIRCMS is a ground-based cloud detection instrument based on uncooled infrared focal plane array (UIRFPA). It can quantitatively measure the distribution of downwelling infrared radiation to detect and classify cloud (Sun, et al., 2008b, 2009a, Sun, et al., 2008). A whole sky image is obtained after calibration and combination (Sun, et al., 2009b, 2009c). In this paper, a method of retrieving CBH according to the downwelling infrared radiation from WSIRCMS is proposed. The accuracy of middle and low CBH from WSIRCMS is discussed compared with data from a laser ceilometer and visual observations.

2　METHODS

CBH can be determined according to the sky infrared brightness temperature that is calculated from the corrected atmospheric downwelling infrared radiance. However, there

are still uncertainties. For example, the accuracy of the corrected downwelling atmospheric infrared radiance is uncertain, and clouds can not been treated as blackbodies at any conditions. What's more, the real-time temperature profiles are difficult to access. Zhang, et al. (2007) studied on the variations of sky infrared brightness temperatures caused by different kinds of clouds and different intensities of aerosols using MODTRAN 4.0 model. It shows that the sky thermal infrared brightness temperature observed on the ground is very sensitive to the variations of CBH for low and middle clouds, therefore as the "clear" sky brightness temperature is known, it can be used to retrieve of CBH. The limit is that real-time atmospheric temperature and humidity profiles should be provided. In order to overcome the shortcoming, Sun, et al. (2009d) proposed a method according to the monotonic relationship between CBH and downwelling infrared radiation. In this paper some simulation results using radative transfer model SBDART (Ricchiazzi, et al., 1998) were presented.

Fig. 1 shows downwelling infrared radiation of different CBH and different optical thickness in the 8—14 μm band using the mid-latitude summer and winter atmospheric model. It shows monotonic relationship between CBH and downwelling infrared radiation, which means for the same optical thickness of cloud, higher cloud-base height leads to less the downwelling infrared radiation, which further ensures to retrieve cloud-base height from downwelling infrared radiation. Furthermore, it seems that, for the same cloud-base height, the radiation increases with optical thickness. How-

ever, if the optical thickness is greater than 8, the radiation does not increase, which suggests that if emissivity cannot be determined well, there should be a large error for detecting the cloud-base height for the optical thin layer cloud.

Downwelling infrared radiance is influenced both by CBH and water vapor content. Fig. 2 shows the 8—14 μm downwelling infrared radiation varying with *PWV* in different visibility and cloud-base height (2.5 km, 6 km, 11 km and clear sky) modeled based on the average 30-year climate sounding data. It

(a) Middle latitude summer model (b) Middle latitude winter model

— *tcloud*=0   — *tcloud*=2   — *tcloud*=5
— - *tcloud*=8   — *tcloud*=10   — *tcloud*=15
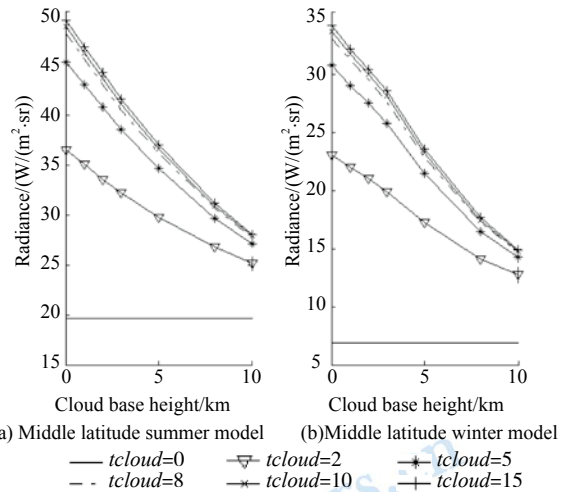
Fig. 1   Downwelling infrared radiation of different CBH and different optical thickness in zenith

(a) *vis*=1 km

(b) *vis*=4 km

(c) *vis*=10 km

(d) *vis*=23 km
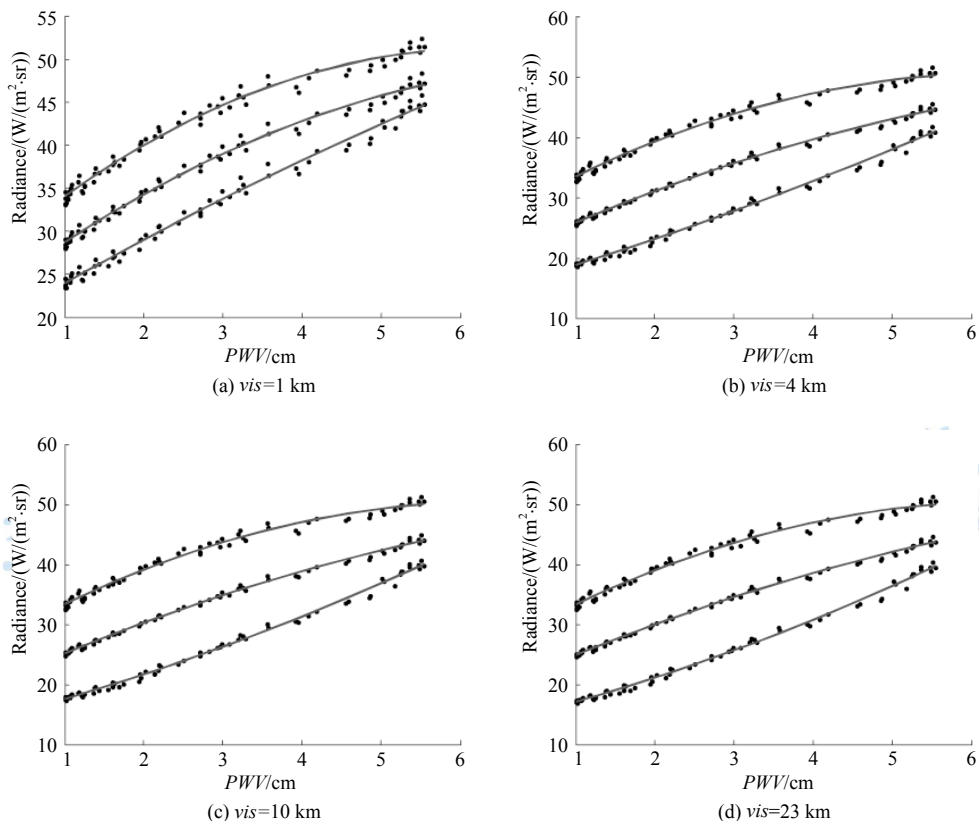
Fig. 2   The relationship between downwelling infrared radiation in zenith and *PWV* (*vis*: visibility)
(Symbol "." represents the simulation value. The upper, middle and lower curves are the fitting curves for cloud-base height of 2.5 km, 6 km and 11 km)

is indicated that, though the profiles of temperature and humidity vary great within a year, a quadratic function relationship as the equation (1) exists between downwelling infrared radiation and *PWV*. In Fig. 2, the symbol "." indicates the value of theoretical simulation. The upper, middle and lower curves are the fitting curves as Eq. (1) at the cloud-base height of 2.5 km, 6 km and 11 km, respectively.

$$L = a \times PWV^2 + b \times PWV + c \qquad (1)$$

where L is downwelling infrared radiance in the 8—14 μm band (W/ (m^2·sr)), *PWV* is the atmospheric precipitable vapor (cm), a, b and c are fitting coefficients.

For different latitudes, different heights can be chosen as separation height thresholds of low, middle and high clouds. In the mid-latitudes, 2.5 km, 6 km and 11 km are chosen as separation heights. The theoretical downwelling radiance at ground from the cloud that cloud-base height is 2.5 km, 6 km and 11 km, which is named respectively as L_L, L_M and L_H, can be calculated by Eq. (1) with real-time *PWV*. The black radiance corresponding to the surface temperature is denoted as L_S. The measured radiance is denoted as L_r. There is no cloud at the pixel if L_r is less than L_H. In other conditions, the cloud-base height can be calculated according to Eq. (2):

$$H = \frac{L_M - L_r}{L_M - L_H} \times (h_H - h_M) + h_M$$
$$L_M > L_r \geq L_H$$
$$H = \frac{L_L - L_r}{L_L - L_M} \times (h_M - h_L) + h_L \qquad (2)$$
$$L_L > L_r \geq L_M$$
$$H = \frac{L_S - L_r}{L_S - L_L} \times h_L$$
$$L_S > L_r \geq L_L$$

where h_H, h_M, and h_L is 11 km, 6 km and 2.5 km, respectively.

3 RESULTS

3.1 Experiment

A comparison test of cloud-base height between WSIRCMS and a laser ceilometer is carried out in Beijing Observatory Station from June 30th to July 8th in 2009. The error of the laser ceilometer is ± 15 m (when cloud-base height is less than 500 m) or ± 10% (when cloud-base height is not less than 500 m). Meanwhile, for comparison, we also estimated cloud-base height using the depression of the dew point as follows (CMA, 2003).

$$H = \frac{t - t_d}{\gamma_d \gamma_\tau} \approx 124(t - t_d) \qquad (3)$$

where H is the cloud-base height, t is the temperature, t_d is the dew point, γ_d is dry air adiabatic lapse rate, which is approximately 0.98 ℃ / 100 m, γ_τ is dry adiabatic lapse rate of the dew point, which is approximately 0.17 ℃ / 100 m. For various reasons, cloud-base heights observed by artificial visual are all 1000 m during the experiment which were excluded from comparison.

Only cloud-base heights near zenith were measured by laser ceilometer, and 13 groups data were collected, which were mainly low and middle clouds.

3.2 Analysis

At 10:00 on 2009-07-01, the environmental conditions are below: the visibility is 10 km, temperature is 30.5 ℃, and relative humidity is 25%. The total cloud cover is about 80 percent with fractocumulus for 60%, and altocumulus translucidus of 20%. Fig. 3 shows the visible light image near the zenith which is dominated by altocumulus translucidus. Fig. 4 shows the value of downwelling infrared radiance measured by WSIRCMS in zenith angles from 0 ° to 20 °, and the thresholds for determining CBH according to real-time weather. It is demonstrated that the radiance varies from 11 W/ (m^2·sr) to 33 W/(m^2·sr) in zenith angles from 0 ° to 20 °. The minimum radiance is larger than the threshold for clear sky but smaller than that of 11 km. The maximum radiance is larger than that of 2.5 km. According to the rules mentioned in Section 2, there was clear sky near the zenith with cloud with base height larger than 2.5 km.

From Table 1, we can see that CBHs retrieved by WSIRCMS are consistent with that measured by laser ceilometer. The maximum difference is 465 m, and the minimum is 98 m, the standard deviation is 259 m. Cloud type is similar with the actual situation according to visual observations. Cloud heights estimated from the
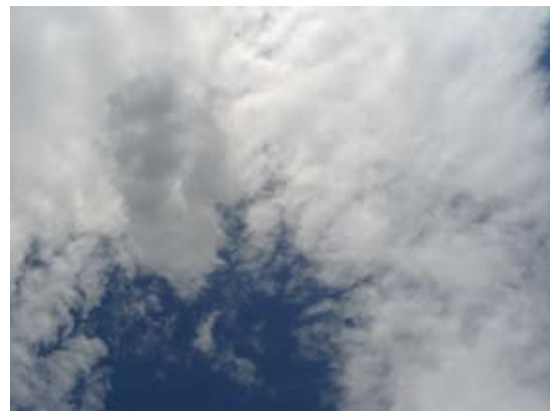
Fig. 3   Visible light image in zenith at 10:00 on 2009-07-01
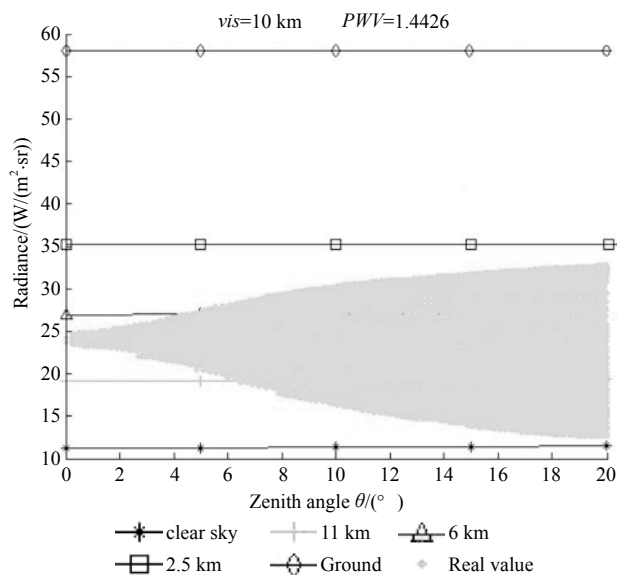
Fig. 4   Downwelling infrared radiance in the zenith angles from 0 ° to 20 ° at 10:00 on 2009-07-01

empirical formula are less accurate, the maximum difference with laser ceilometer is up to 478 m, the minimum difference is 50 m, and the standard deviation is 318 m. The average cloud-base height measured by laser ceilometer is 2806 m, and 2913 m by WSIRC-MS, respectively. The average difference is around 107 m. The average cloud-base height estimated from the empirical formula is up to 3090 m, and the average difference with laser measurement is 284 m. It seems that CBHs retrieved from WSIRCMS are more close to the real value than that from empirical formula.

Table 1　CBHs determined by laser ceilometer, WSIRCMS and empiri cal formula /m

Time	Laser ceilom-eter	WSIRCMS	Empirical formula
2009-06-30 T 14:30	3150	3052	3543
2009-06-30 T 15:00	3309	3676	3787
2009-06-30 T 15:30	3203	2995	3322
2009-06-30 T 16:00	3179	3412	3434
2009-06-30 T 17:30	3208	3523	3660
2009-06-30 T 18:00	3288	3499	3534
2009-07-01 T 10:00	2475	2802	2755
2009-07-01 T 11:00	2471	2936	2853
2009-07-01 T 11:30	2580	2770	2933
2009-07-01 T 12:00	2550	2432	2939
2009-07-01 T 12:30	2697	2498	2849
2009-07-01 T 13:00	2592	2361	2840
2009-07-01 T 13:30	1773	1913	1723

4　CONCLUSIONS

There are many factors which may influence the accuracy of CBH remote sensing on the use of downwelling infrared radiation. In this paper, a method for retrieving CBH is proposed according to the monotonic relationship between CBH and downward infrared radiance based on the analysis of results of radiative transfer simulation. The CBHs retrieved from WSIRCMS were compared with data measured by laser ceilometer and estimates from empirical formula. The results show high accuracy of the middle and low CBH determined according to the proposed method with the average error of 107 m. The method can both be used to acquire CBH in zenith and to determine CBH in different elevation angles.

Atmospheric temperature and humidity profiles vary in different areas and seasons, which may change the statistical relationship between CBH and downwelling infrared radiation. It is necessary to find how the fitting coefficients are depended on locations and seasons. Experiments on the proposed method for estimation CBH of high cloud have been carrying out, and a preliminary analysis is conducted. It can provide more information such as 3D cloud structure combining CBHs generated by ground infrared detection with cloud top heights retrieved from satellite.

REFERENCES

China Meteorological Administration. 2003. Criterion of Surface Meteorological Observation. Beijing: China Meteorological Press: 15–16

Genkova I, Long C N, Besnard T and Gillotay D. 2004. Assessing cloud spatial and vertical distribution with infrared cloud analyzer. New Mexico: Fourteenth ARM Science Team Meeting Proceedings: 22–26

Huo J and Lv D R. 2002. Preliminary study on cloud-cover using an all-sky digital camera. Journal of Nanjing Institute of Meteorology, 25(2): 242–246

Long C N and DeLuisi J J. 1998. Development of an automated hemispheric sky imager for cloud fraction retrievals. In: Proc. 10th Symp. on Meteorological Observations and Instrumentation, Phoenix, Arizona

Ricchiazzi P, Yang S R, Gautier C and Sowle D. 1998. SBDART: A research and teaching software tool for plane-parallel radiative transfer in the Earth's atmosphere. Bulletin American Meteorological Society, 79(10): 2101–2114

Shields J E, Johnson R W, Karr M E and Wertz J L. 1998. Automated day/night whole sky imagers for field assessment of cloud cover distributions and radiance distributions. Tenth Symposium on Meteorological Observations and Instrumentation

Shaw J A, Thurairajah B, Edqvist E and Mizutani K. 2002. Infrared cloud imager deployment at the north slope of Alaska during early 2002. 12th ARM Science Team Meeting

Sun X G, Sun X J, Niu Z C and Gao T C. 2008. A method of capturing whole-sky nephogram and it's arithmetic actualization. Scientia Meteorologica Sinica, 28(3): 338–341

Sun X J. 2009. Study on the ground-based infrared remote sensing of whole sky cloud. Beijing: Institute of Physics, Beijing University

Sun X J, Gao T C, Zhai D L, Zhao S J and Lian J G. 2008a. Whole sky infrared cloud measuring system based on the uncooled infrared focal plane array. Infrared and Laser Engineering, 37(5): 761–764

Sun X J, Liu J, Zhao S J, Zhai D L and Mao J T. 2008b. Radiometric calibration model of the uncooled infrared focal plane array. Journal of PLA University of Science and Technology (Natural Science Edition), 9(4): 399–403

Sun X J, Liu J and Mao J T. 2009a. Vicarious calibration of the sensor of whole sky infrared cloud measuring system. Journal of Infrared and Millimeter Waves, 28(1): 54–57

Sun X J, Liu L, Gao T C, Zhao S J, Liu J and Mao J T. 2009b. Cloud classification of the whole sky infrared image based on the fuzzy uncertainty texture spectrum. Journal of Applied Meteorological Science, 20(2): 157–163

Sun X J, Liu L, Gao T C and Zhao S J. 2009c. Classification of whole sky infrared cloud image based on the LBP operator. Transactions of Atmospheric Sciences, 32(4): 490–497

Zhang W X, Lü D R and Chang Y L. 2007. A feasibility study of cloud base height remote sensing by simulating ground-based thermal infrared brightness temperature measurements. Chinese Journal of Geophysics, 50(2): 354–363

中低云云底高的地基红外遥感的初步分析

孙学金，秦超，秦健，刘磊，胡渝宁

解放军理工大学 气象学院，江苏 南京 211101

摘　要： 在辐射传输模拟结果分析的基础上，提出利用云底高与下行红外辐射之间的单调关系进行云底高遥感反演的算法，并结合激光测云仪云底高实测数据对算法进行了初步验证。结果表明，该算法对中低云云底高反演的平均误差为107 m，具有较高的准确性。

关键词： 云底高，红外遥感，下行红外辐射，地基遥感，激光测云仪

中图分类号： P407.6　　　　**文献标志码：** A

1　引　言

　　云是地气系统辐射收支的主要调节者，是影响地气系统辐射平衡的重要因素。长期以来，云的地基观测仍然以人工目测为主。从20世纪60年代以后，利用气象卫星进行云的遥感成为重要的观测手段，取得的大量云观测资料，成为研究云的全球分布和变化规律的重要基础数据。尽管卫星遥感可获得全球分布、昼夜连续的云资料，但由于其空间分辨率以及对云底和多层云的下层云的观测能力的限制，仍然不能完全满足大气科学研究的需要。研究表明，云底高度是影响地球长波辐射能量收支的重要因子之一。此外，卫星遥感数据的准确性也需要地面云观测资料的验证。因此，地基的云观测仍然是必要和重要的云观测手段之一。

　　目前，以人工目测为主要手段的地基云观测方法，并不足以提供时间分辨率高、昼夜准确性一致和客观的云观测资料。激光测云雷达常用于测量与云有关的参数，它具有单色性好、定向性强、相干性高和体积小等特点，但激光雷达仅为单点观测，不能全天候的进行测量，也不能反映云量等其他信息，而且受气溶胶影响较大，业务使用受到一定限制。随着数字技术的发展，研制出各种可见光数字式成像仪，如总天空成像仪TSI(Long 和 DeLuisi，1998)，全天空成像仪WSI(Shields 等，1998)和全天空数字相机(Huo和Lv，2002)等。可见光成像测云的主要局限在于无法获得夜间的云量或者由于白天夜间云的识别算法的不同而导致测量结果的昼夜准确性有差异。近十几年来，随着红外测量技术的发展，利用热红外进行云的地基遥感得到了发展，如红外云分析仪ICA(Genkova 等，2004)，红外云成像仪ICI(Shaw 等，2002)和全天空红外测云系统(孙学金 等，2008a)。地基红外遥感技术白天夜间均可以对云进行成像观测，不仅可以获得云量的资料，还可以进一步反演获得云底高度。

　　全天空红外测云系统(WSIRCMS)是基于非制冷红外焦平面阵列的地基测云仪器，通过对非制冷红外焦平面阵列的定标处理和扫描拼图处理(孙学金 等，2008b，2009a，孙晓刚 等，2008)，可对全天空下行红外辐射分布进行定量测量，进而实现全天空云的遥感测量，识别出云类(孙学金 等，2009b，2009c)。本文利用WSIRCMS数据，开展了利用下行红外辐射进行云底高的地基遥感研究，并结合激光测云仪以及人工观测资料，对中低云云底高的遥感结果进行了初步验证。

2　云底高地基红外遥感算法

云底高的反演可先从传感器测量的下行红外辐射中对大气下行红外辐射进行修正后，得到云底的下行红外辐射，求出云底亮温，然后再根据亮温、温湿廓线反演云底高。由于大气下行红外辐射修正值精度、云为黑体的不确定性以及实时气温廓线的获取困难等，使得云底高的反演存在诸多的不确定性。章文星等人(2007)利用MODTRAN4.0模式研究了不同强度和不同类型气溶胶情况下，晴空和不同云底高度云所形成的天空红外亮温随地面天顶角的变化，指出利用亮温可进行云底高的遥感。其不足之处在于需要知道实时的温湿廓线并进行大气修正。为了在未知温湿廓线的情况下，能利用下行红外辐射反演云底高，孙学金等人(2009)提出了利用云底高与下行红外辐射之间的单调对应关系进行云底高反演的算法。

图1为利用SBDART(Ricchiazzi 等，1998)模式，在中纬度夏季和冬季大气模式下模拟计算的不同高度、不同光学厚度时的8—14 μm波段的下行红外辐射。从图1可以看出，对于同一光学厚度的云，随着云底高的增加，地面所接收到的下行红外辐射越小，具有单调下降

关系，这为利用下行红外辐射进行云底高遥感提供了基础。对于同一云底高，随着光学厚度的增大，辐射增大，但当光学厚度大于8以后，辐射几乎不再增大，这表明对于光学薄层的云，若不能较好地确定云的比辐射率，则对云底高的反演带来较大的误差。

下行红外辐射不仅与云底高有关，还与大气水汽含量有关。图2为利用30年气候平均探空资料，模拟计算的全年不同能见度下晴空以及云底高为2.5 km、6 km、

(a) 中纬度夏季模式　　　(b) 中纬度冬季模式

—— tcloud=0　　▽ tcloud=2　　* tcloud=5
-- tcloud=8　　× tcloud=10　　+ tcloud=15
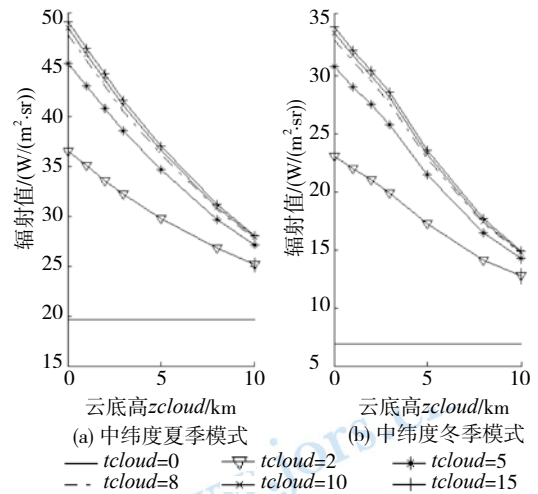
图1　不同光学厚度、云底高情况下天顶方向下行红外辐射值

(a) vis=1 km

(b) vis=4 km

(c) vis=10 km

(d) vis=23 km
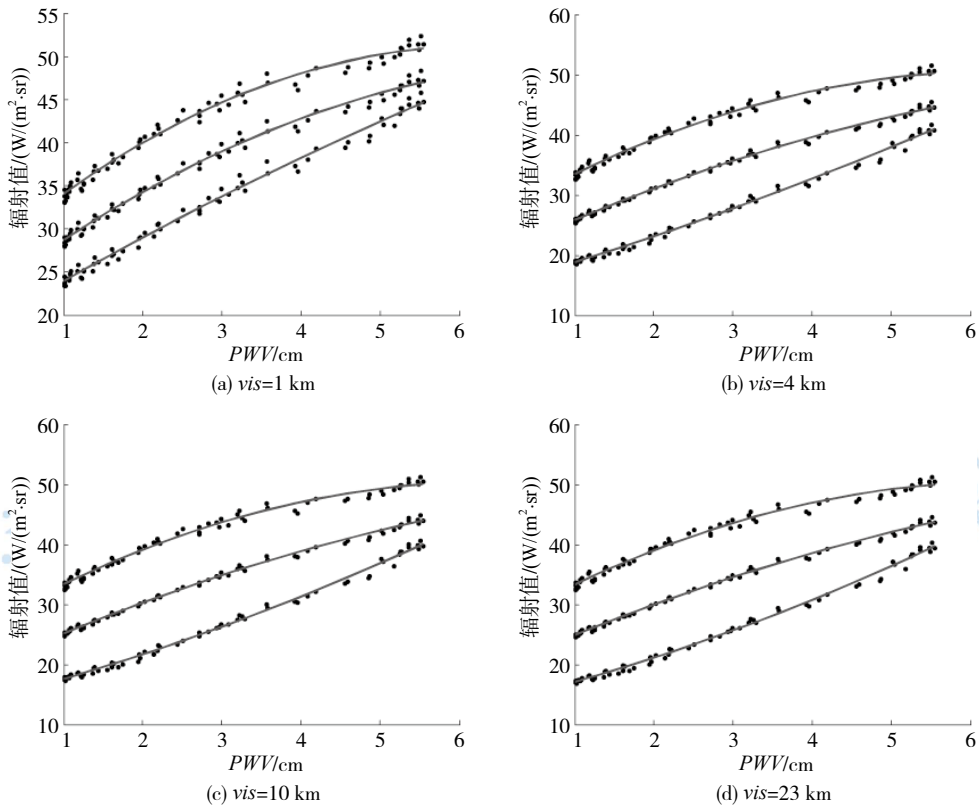
图2　天顶方向下行红外辐射值与PWV的关系

(·为模拟计算值；上、中和下3条曲线分别为云底高2.5 km、6 km和11 km的拟合曲线；vis为能见度)

11 km时8—14 μm波段的下行红外辐射随*PWV*变化的情况。从图2可以发现，尽管一年中温湿廓线变化较大，但下行红外辐射与*PWV*之间具有如式(1)所示的二次函数关系。图中"·"表示理论模拟值，而上、中和下3条曲线分别为利用式(1)在云底高为2.5 km、6 km和11 km的拟合曲线，由于气候平均探空资料是按旬分08：00和20：00两个时次统计的，因而图中2个时次的拟合曲线稍有些不重合，但变化不大。

$$L = a \times PWV^2 + b \times PWV + c \tag{1}$$

式中，*L*为8—14 μm波段大气下行红外辐射(W/(m²·sr))，*PWV*为大气可降水量(cm)，*a*、*b*、*c*为拟合系数。

对于不同纬度地区可选择合适的云底高作为分界高度进行分段拟合，在中纬度地区常将2.5 km、6 km和11 km时作为低中高云的分界高度。这样，若实时测出*PWV*，则可利用式(1)分别计算出2.5 km、6 km和11 km时的辐射值，分别记为L_L、L_M和L_H。设近地面气温对应的辐射值为L_S，实测的辐射值为L_r。若L_r小于L_H，则可判别此像元无云。而云底高则可按式(2)计算：

$$H = \frac{L_M - L_r}{L_M - L_H} \times (h_H - h_M) + h_M$$
$$L_M > L_r \geq L_H$$
$$H = \frac{L_L - L_r}{L_L - L_M} \times (h_M - h_L) + h_L \tag{2}$$
$$L_L > L_r \geq L_M$$
$$H = \frac{L_S - L_r}{L_S - L_L} \times h_L$$
$$L_S > L_r \geq L_L$$

式中，h_H、h_M和h_L分别是指11 km、6 km和2.5 km。

3   试验结果

3.1   实验介绍

2009-06-30—07-08在北京市观象台进行了WSIRC-MS与手持式激光测云仪云底高测量结果对比试验。手持式激光测云仪云底高度测量误差±15 m(云底高小于500 m时)或±10%(云底高不小于500 m时)。同时，为了进行比较，还利用地面温度露点差估算了云底高度，估算公式(中国气象局，2003)为：

$$H = \frac{t - t_d}{\gamma_d \gamma_\tau} \approx 124(t - t_d) \tag{3}$$

式中，*H*为云底高，*t*为气温，t_d为露点温度，γ_d为干空气的绝热直减率，近似为0.98℃/100 m，γ_τ为露点温度在干绝热阶段的直减率，近似为0.17℃/100 m。

由于各种原因，实验期间人工云底高观测结果都为1000 m，因而未与人工云底高观测结果进行比较分析，人工观测的云状结果作为参考。

为了便于比较，只对天顶附近的云底高度进行了激光测量，共采集到有激光云底高度的数据13组时次，主要是中低云。

3.2   结果与分析

2009-07-01上午10：00能见度为10 km，气温30.5℃，相对湿度25%，天空为6成碎积云，2成透光高积云，总云量为8成。图3为相应时次所拍摄的天顶附近可见光图像，以透光高积云为主。图4是该时次WSIRCMS实测天顶角0°—20°范围内不同方位的下行红外辐射值和根据当时实况确定的不同云底高度的阈值。在天顶角0°—20°范围内，辐射值在11—33 W/(m²·sr)之间变化，其最小值在晴空阈值线以上，11

图3   2009-07-01 T 10:00天顶方向天空状况
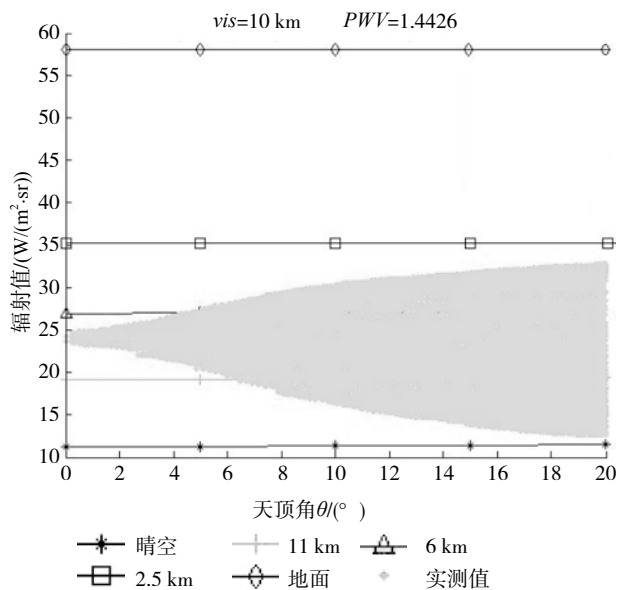
图4   2009-07-01 T 10:00天顶角20°范围内实测下行红外辐射值及阈值

km阈值线下，最大值在2.5 km阈值线以下。按照前述判别法则，当时天顶处附近存在晴空区域，云底高大于2.5 km，与当时的实际天空状况符合。

表1是实验时段激光测云仪、WSIRCMS反演和公式计算的云底高结果。从表1可看出WSIRCMS反演的中低云云底高基本与激光测云仪所测结果相符，也与当时天空出现的云状基本一致。WSIRCMS反演云底高与激光实测云底高之间的最大差值为465 m，最小差值为98 m，标准偏差为259 m；而公式计算的云底高与激光实测云底高之间的最大差值为478 m，最小差值为50 m，标准偏差为318 m。进一步分析可知，激光实测云底高平均值为2806 m，WSIRCMS反演的云底高平均值为2913 m，与激光实测云底高相差107 m；而公式估算的云底高平均值为3090 m，与激光实测云底高相差284 m。可见WSIRCMS反演的云底高要比公式估算的云底高更接近于激光实测云底高。

表1   激光实测、WSIRCMS反演与公式估算的云底高 /m

时间	激光实测	WSIR CMS	公式估算
2009–06–30 T 14:30	3150	3052	3543
2009–06–30 T 15:00	3309	3676	3787
2009–06–30 T 15:30	3203	2995	3322
2009–06–30 T 16:00	3179	3412	3434
2009–06–30 T 17:30	3208	3523	3660
2009–06–30 T 18:00	3288	3499	3534
2009–07–01 T 10:00	2475	2802	2755
2009–07–01 T 11:00	2471	2936	2853
2009–07–01 T 11:30	2580	2770	2933
2009–07–01 T 12:00	2550	2432	2939
2009–07–01 T 12:30	2697	2498	2849
2009–07–01 T 13:00	2592	2361	2840
2009–07–01 T 13:30	1773	1913	1723

4   结   论

利用下行红外辐射进行云底高的遥感反演的准确度受到许多因素的影响，本文在辐射传输模拟结果分析的基础上，提出了利用云底高与下行红外辐射之间的单调关系进行云底高遥感反演的算法，并结合激光测云仪云底高实测数据对算法进行了初步验证，结果表明该算法对中低云云底高反演的平均误差为107 m，具有较高的准确性。由于全天空红外测云系统具有对不同方位和仰角云体的探测能力，还可进一步提取云厚信息，为研究云的垂直发展提供了一种新的手段。

由于不同地区大气温湿廓线的差异性，云底高

与下行红外辐射之间的统计关系随地区和季节差异较大，需要根据不同地点和季节分别统计拟合系数。利用该算法对高云云底高的探测能力的验证正在试验中，初步分析表明对高云云底高也具有较高的准确性。综合利用地基红外云底高的探测数据与卫星对云顶高的探测数据，必将提高对云的三维立体认识。

参考文献(References)

China Meteorological Administration. 2003. Criterion of Surface Meteorological Observation. Beijing: China Meteorological Press: 15–16

Genkova I, Long C N, Besnard T and Gillotay D. 2004. Assessing cloud spatial and vertical distribution with infrared cloud analyzer. New Mexico: Fourteenth ARM Science Team Meeting Proceedings: 22–26

霍娟, 吕达仁. 2002. 全天空数字相机观测云量的初步研究. 南京气象学院学报, 25(2): 242–246

Long C N and DeLuisi J J. 1998. Development of an automated hemispheric sky imager for cloud fraction retrievals. In: Proc. 10th Symp. on Meteorological Observations and Instrumentation, Phoenix, Arizona

Ricchiazzi P, Yang S R, Gautier C and Sowle D. 1998. SBDART: A research and teaching software tool for plane-parallel radiative transfer in the Earth's atmosphere. Bulletin American Meteorological Society,79(10): 2101–2114

Shields J E, Johnson R W, Karr M E and Wertz J L. 1998. Automated day/night whole sky imagers for field assessment of cloud cover distributions and radiance distributions. Tenth Symposium on Meteorological Observations and Instrumentation

Shaw J A, Thurairajah B, Edqvist E and Mizutani K. 2002. Infrared cloud imager deployment at the north slope of Alaska during early 2002. 12th ARM Science Team Meeting

孙晓钢, 孙学金, 牛珍聪, 高太长. 2008. 全天空云图获取的一种方式及算法实现. 气象科学, 28(3): 338–341

孙学金.2009. 云的地基全天空红外遥感研究.北京:北京大学物理学院

孙学金, 高太长, 翟东力, 赵世军, 练进根. 2008a. 基于非制冷红外焦平面阵列的全天空红外测云系统. 红外与激光工程, 37(5): 761–764

孙学金, 刘剑, 赵世军, 翟东力, 毛节泰. 2008b. 非致冷红外焦平面阵列的辐射定标模型. 解放军理工大学学报(自然科学版), 9(4): 399–403

孙学金, 刘剑, 毛节泰. 2009a. 全天空红外测云系统辐射传感器的替代定标. 红外与毫米波学报, 28(1): 54–57

孙学金, 刘磊, 高太长, 赵世军, 刘剑, 毛节泰. 2009b. 基于模糊纹理光谱的全天空红外图像云分类. 应用气象学报, 20(2): 157–163

孙学金, 刘磊, 高太长, 赵世军. 2009c. 基于LBP算法的全天空红外云图的分类研究. 大气科学学报, 32(4): 490–497

章文星, 吕达仁, 常有礼. 2007. 地基热红外亮温遥感云底高度可行性的模拟研究. 地球物理学报, 50(2): 354–363

中国气象局. 2003. 地面气象观测规范. 北京: 气象出版社: 15–16